9456–9470 *Nucleic Acids Research, 2018, Vol. 46, No. 18* *Published online 24 July 2018*
doi: 10.1093/nar/gky659

TIP60 represses activation of endogenous retroviral elements

Deepa Rajagopalan[1,2], Roberto Tirado-Magallanes[1], Shreshtha Sailesh Bhatia[1], Wen Shiun Teo[1], Stephanie Sian[1], Shainan Hora[1,2], Kwok Kin Lee[1], Yanzhou Zhang[1], Shweta Pradip Jadhav[1], Yonghui Wu[3], Yunn-Hwen Gan[2], Neerja Karnani[2,3], Touati Benoukraf[1] and Sudhakar Jha[1,2,*]

[1]Cancer Science Institute of Singapore, National University of Singapore, Singapore 117599, [2]Department of Biochemistry, Yong Loo Lin School of Medicine, National University of Singapore, Singapore and [3]Singapore Institute for Clinical Sciences, A* STAR, Singapore

Received January 06, 2018; Revised July 07, 2018; Editorial Decision July 09, 2018; Accepted July 11, 2018

ABSTRACT

TIP60 is a lysine acetyltransferase and is known to be a haplo-insufficient tumor suppressor. TIP60 downregulation is an early event in tumorigenesis which has been observed in several cancer types including breast and colorectal cancers. However, the mechanism by which it regulates tumor progression is not well understood. In this study, we identified the role of TIP60 in the silencing of endogenous retroviral elements (ERVs). TIP60-mediated silencing of ERVs is dependent on BRD4. TIP60 and BRD4 positively regulate the expression of enzymes, *SUV39H1* and *SETDB1* and thereby, the global H3K9 trimethylation (H3K9me3) level. In colorectal cancer, we found that the loss of TIP60 de-represses retrotransposon elements genome-wide, which in turn activate the cellular response to pathogens, mediated by STING, culminating in an induction of Interferon Regulatory Factor 7 (IRF7) and associated inflammatory response. In summary, this study has identified a unique mechanism of ERV regulation in cancer cells mediated by TIP60 and BRD4 through regulation of histone H3 K9 trimethylation, and a new tumor suppressive role of TIP60 *in vivo*.

INTRODUCTION

HIV-1 TAT Interactive Protein (TIP60) is a lysine acetyltransferase that belongs to the MYST (Moz, Ybf2/Sas3, Sas2 and TIP60) family of acetyltransferases and is capable of acetylating both histone and non-histone proteins (1,2). TIP60 is involved in the DNA damage response. Acetylation of ataxia telangiectasia mutant (ATM) by TIP60 at K3016 activates the downstream signaling cascade to ATM (3). In addition, TIP60 acetylates p53 and this recruits p53 selectively to the promoters of pro-apoptotic genes such as *BAX* and *PUMA* (4,5). TIP60 is known to acetylate histones H2 and H4 conventionally, thereby activating transcription through remodeling chromatin state (6). TIP60 also acts as a coactivator for a variety of transcription factors such as MYC and androgen receptor, being recruited by these factors to either acetylate histones or the factors themselves to activate transcription (7–9). However, emerging evidence indicates an unconventional repressive function for this acetyltransferase. In the context of human papillomavirus (HPV)-induced cervical cancer, TIP60 can acetylate histones on the promoter of the viral oncogene, E6, resulting in recruitment of bromodomain-containing protein 4 (BRD4) and repression of gene expression (10). Adenoviral E1A promoter as well as cellular genes such as *DKC* and *TERT* (10–12) are also known to be repressed by TIP60. TIP60 has been characterized to be a bonafide haplo-insufficient tumor suppressor (13). Consistent with this observation, TIP60 expression is downregulated in various tumor types such as breast and colorectal cancers (13,14). Reactivation of TIP60 in cervical cancer cell lines is shown to cause a remarkable decrease in tumor formation *in vivo* and colony formation ability *in vitro* (15), emphasizing the role of TIP60 as a tumor suppressor. However, the precise molecular mechanisms regulated by TIP60 to achieve tumor suppression in different cancers has yet to be characterized. TIP60 nuclear staining is reduced in mammary samples from carcinoma *in situ* as well as in invasive carcinoma (13), suggesting that TIP60 downregulation is an early event in the tumorigenesis process. The role of TIP60 in the early stages of tumor development has not been identified.

Tumorigenesis is a multi-step process that occurs through a series of mutations in cancer-associated genes which could be oncogenes, tumor suppressor genes or genes in which dis-

*To whom correspondence should be addressed. Tel: +65 66012402; Fax: +65 68739664; Email: csisjha@nus.edu.sg

ruption could result in genomic instability. It also involves heterogeneous populations of cancer stem cells (16,17). A plausible cause for these mutations are insertional mutation events caused by transposition events. Forty-two percent of the human genome consists of mobile genetic elements, including transposable elements with their two subclasses: retrotransposons and DNA transposons (18,19). Based on the presence of long terminal repeats (LTRs) flanking their sequences, retrotransposons are further classified into LTR (members of human endogenous retroviruses, HERV) and non-LTR elements (long interspersed nuclear elements, LINE and short interspersed nuclear elements, SINE) (18,20). The expression of these transposable elements is tightly regulated in a tissue-specific manner by being co-regulated with the tissue type defining host genes (21,22). The repressive mechanisms that regulate retrotransposon amplification include DNA methylation by enzymes such as DNMT (DNA methyltransferase)1 and to a lesser extent DNMT3a, DNMT3b as well as histone methytransferases such as SETDB1 depending on the stage of development (22–26). However, the intricate details remain to be characterized. Detection of endogenous retroviral (ERVs) element intermediates like cytosolic DNA (c-DNA) has been associated with the pathogenesis of autoimmune diseases like Aicardi-Goutières syndrome (AGS) (20) as well as in different cancers such as melanoma and teratocarcinomas (27,28). ERVs, when de-repressed by treatment with DNA demethylating agents in colorectal cancer as well as in melanoma, trigger detection by the cytosolic sensors and mimic pathogenic stimuli such as pathogen associated molecular patterns (PAMPs), leading to sensitization to immune therapy (29,30). However, the stable silencing mechanisms of ERVs in cancer cells remain largely unknown. Retrotransposons replicate via an RNA intermediate, subsequently leading to the production of c-DNA by reverse transcription, and are known to cause double stranded breaks in DNA, leading to mutagenesis and cancer (18,31). Since the life cycle of retroviral elements involves nucleic acid intermediates, these have the potential to act as ligands for cellular pattern recognition receptors (PRRs) (32). These cellular receptors equip the cells to deal with invading pathogens and are an integral component of the innate immune system. The cellular PRRs are classified into two categories based on their intracellular localization: cytosolic receptors like RIG-I and MDA-5 for detection of cytosolic RNA (c-RNA) and c-GAS for c-DNA as well as transmembrane PRRs which include the various classes of Toll-like receptors (TLRs) (33–35). The signaling through these receptors culminates in the activation of a multitude of transcription factors including the different interferon regulatory factors (IRF) and nuclear factor-κB (NF-κB) which alter the gene expression profile of the cell, inducing pro-inflammatory cytokines as well as interferons, to combat the infection (36).

Based on TIP60 downregulation in early stages of cancer (13) and the innate immune gene signature associated with TIP60 depletion in our study, we speculated that TIP60 could be implicated in tumor-associated inflammation by stable silencing of transposable elements. This study has identified a novel mechanism of activation of an interferon response in cancer cells upon downregulation of TIP60. It involves re-activation of specific endogenous retroviral elements, which are recognized by the c-DNA adaptor protein STING, and results in the induction of *IRF7* expression and associated inflammatory response. Mechanistically, TIP60 positively regulates the expression of Histone H3 K9 trimethylating (H3K9me3) enzymes, *SUV39H1* and *SETDB1* and loss of TIP60 also results in a global decrease in H3K9me3. Stable overexpression of TIP60 in colorectal cancer cells reduces the colony formation ability *in vitro* as well as tumor growth *in vivo* and results in repression of the ERV expression, suggesting a strong link between decreased TIP60 expression, ERV reactivation and tumor growth.

MATERIALS AND METHODS

Cell culture

293T cells (ATCC® CRL-3216™), C-33A cells (ATCC® HTB-31™), HT-29 (ATCC® HTB-38™), SW480 (ATCC® CCL228™) and SW620 (ATCC® CCL-227™) were cultured in Dulbecco's modified Eagle's medium (DMEM) high glucose (Sigma Cat. No. D-5796), HCT116 cells (ATCC® CCL-247™) in RPMI 1640 Media (HyClone Cat. No. SH30027.01) with 10% fetal bovine serum (Sigma Cat. No. F-7524), 1% penicillin streptomycin (Gibco Cat. No. 15140-122) at 37°C and 5% CO_2. MCF10A cells (ATCC CRL-10317™) were cultured in DMEM/F12 (1:1) media (Gibco, Cat. No. 11330-032) with 5% horse serum (Gibco, Cat. No. 16050-122), 1% penicillin streptomycin (Gibco, Cat. No. 15140-122), 20 ng/ml epithelial growth factor (Peprotech), 0.5 mg/ml hydrocortisone (Sigma, Cat. No. H-0888), 100 ng/ml cholera toxin (Sigma, Cat. No. C-8052) and 10 μg/ml insulin (Sigma Cat. No. I-1882). Stable cell lines used in the study were generated by retroviral infection as described below.

Generation of stable cell lines

The retrovirus was generated by transfecting 5×10^6 293T cells with the plasmids (MSCV, MSCV-TIP60 wild-type (TIP60WT) and siRNA-resistant TIP60 wild-type (TIP60*WT) using Lipofectamine 2000 (Invitrogen, Cat. No. 52887) according to manufacturer's protocol. Virus was harvested after 72 h of transfection and was used to infect 2×10^6 HCT116 cells with polybrene (Sigma, Cat. No. 107689) reagent (0.4 mg/ml). After 6 h, media-containing virus was replaced with growth media. After 24 h, puromycin was added in growth media for selection. The cells were selected until the mock transfected cells died and this was continued for an additional 2 weeks for stocks to be made.

siRNA transfection

A commercially available siRNA targeting TIP60 (siTIP60B) was purchased (Sigma Aldrich, SASI_Hs01_00073301) and used in experiments to reduce the possibility of off-target effects. The sequence of the other customized siRNA used for the rescue experiments is described in Supplementary Table S1. Briefly, one million cells were seeded in a 10-cm plate and were used for transfection along with 15 μl Lipofectamine RNAiMax (Invitrogen,

Cat. No. 56532) following the manufacturer's protocol. Six hours post transfection, the transfection mixture was replaced with growth medium and the cells were harvested 72 h after transfection for further analysis. All other proteins used in this study were depleted by transiently transfecting siRNA, targeting the open reading frame of these proteins and the sequences used are described in Supplementary Table S1 (10,37,38).

RNA isolation

Cells were harvested and total RNA was isolated using TRIZOL reagent (Life Technologies, Cat. No. 15596-026) according to manufacturer's protocol.

Real time PCR (RT-PCR) analysis

The total RNA was converted into complimentary DNA (cDNA) using iSCRIPT cDNA synthesis kit (Bio-Rad Cat. No. 170-8891). This served as a template for RT-PCR analysis using iTaq Universal SYBR Green Supermix (Bio-Rad Cat. No. 172-5124) on an Applied Biosystems 7500 Fast Real Time PCR system. Results were analyzed and represented as fold change, normalized to *GAPDH*. The primers used are specified in the primer list (Supplementary Table S2).

Western blot analysis

Proteins were separated on SDS-PAGE gel, transferred onto a nitrocellulose membrane, and detected with primary antibody (in 3% milk in TBST) against α-Actinin (B-12, Santa Cruz, Cat. No. sc-166524, 1:1000), FLAG (Sigma, Cat. No. F7425, 1:1000), IRF-7 (SantaCruz Cat. No. sc-74472, 1:500), BRD4 (Bethyl laboratories, Cat. No. A301-985A100, 1:1000), STING (Cell Signaling Technology, D2P2F, Cat. No. 13647, 1:1000) TIP60 (generated in the lab 1:500), histone H3K9me3 (Cell Signaling, Cat. No. 13969S) and histone H3 (Cell Signaling, Cat. No. 4499S).

Chromatin immunoprecipitation

ChIP was performed following the protocol as described (10). Briefly, seventy-two hours after knockdown, cells were cross-linked with 1% formaldehyde for 10 min at room temperature. The cells were lysed using SDS Lysis buffer for ChIP (1% SDS, 10 mM EDTA, 50 mM Tris-HCl pH 8). The lysate was then sonicated for 25 cycles at 30% amplitude (15 s ON and 45 s OFF). The sonicated samples were then diluted in ChIP dilution buffer (0.01% SDS, 1% Triton-X-100, 1.2 mM EDTA, 16.7 mM Tris–HCl pH 8, 167 mM NaCl) and used for the immunoprecipitation with anti-AcH2A.Z (Abcam, Cat.No. Ab 18262), H2A.Z antibodies (Abcam, Cat.No. Ab 4174), anti-BRD4 (Cell Signaling, Cat. No. 13440S) or FLAG-M2 (Sigma-Aldrich A2220) beads. After an over-night incubation with antibody, the bound DNA was washed sequentially with low salt wash buffer (0.1% SDS, 1% Triton X 100, 2 mM EDTA, 20 mM Tris–HCl pH 8, 150 mM NaCl), high salt wash buffer (0.1% SDS, 1% Triton X-100, 2 mM EDTA, 20 mM Tris–HCl pH 8, 500 mM NaCl), LiCl wash buffer (0.25 M LiCl, 1% NP40, 1%deoxycholate, 1 mM EDTA, 10 mM Tris–HCl pH 8) and TE wash buffer (10 mM Tris–HCl pH 8, 1 mM EDTA) to remove non-specific sequences and eluted in the elution buffer (84 mg $NaHCO_3$, 1 ml 10% SDS, 9 ml H_2O). Then the samples were reverse cross-linked using NaCl at 65°C overnight. The eluted DNA was purified and used for qPCR. qPCR was performed as described above using primers described in Supplementary Table S3.

Colony formation assay

One thousand five hundred cells per well of HCT116-MSCV or HCT116-TIP60-WT were seeded in a 6-well plate for colony formation assay. Ten days after, they were fixed with 20% Methanol and stained with Crystal Violet. Colonies were quantified using ImageJ software.

Xenograft experiments

Six-week-old NOD/SCID mice obtained from Invivos (Singapore) were randomly distributed and HCT116-MSCV or HCT116-TIP60 cells in 100 μl of serum-free RPMI medium at a concentration of 1×10^7 cells/ml supplemented with BD Matrigel matrix (BD Biosciences Cat. No. 354234, Bedford, MA, USA) and were injected subcutaneously into the right or the left flank of the mice. Tumors were examined at indicated times and total tumor volume was recorded. Tumor volume (mm^3) was calculated using the formula: volume (V) = (π/6) width (W)(2) × length (L). The National University of Singapore Institutional Animal Care and Use Committee has approved the work done in this study in accordance with the National Advisory Committee for Laboratory Animal Research Guidelines (Guidelines on the Care and Use of Animals for Scientific Purposes) in facilities licensed by the Agri-Food and Veterinary Authority of Singapore, the regulatory body of the Singapore Animals and Birds Act.

RNA-Seq analysis

STAR (39) was used to map the sequencing reads to the human genome (UCSC hg38) index generated with the gencode annotation (V26). DESeq2 was used to perform the differential expression analysis (40).

Quantification of repetitive element expression

Bowtie (41) was used to align the RNA-seq paired reads to hg38 allowing only unique mapped reads (-m1) and output the multimapping reads to a fastq file with the –max option. The resulting sam with uniquely aligned reads and fastq with multimapped reads were used to quantify repetitive element abundance with RepEnrich (42) using hg38 RepeatMasker annotation as the reference for the repetitive elements. The resulting fragment count files were normalized by the number of reads aligned in each RNA-seq library, the difference in fragment counts and statistical analysis between repetitive elements in siControl and siTIP60 was calculated using DESeq2.

Statistical analysis

All statistical analyses were performed using unpaired two-tailed Student's *t*-test. Error bars indicate standard error of mean (SEM) for the indicated number of biological repeats. Significance is represented as $*P < 0.05$, $**P < 0.01$, $***P < 0.001$.

RESULTS

Depletion of TIP60 shows an inflammatory response gene signature

TIP60 expression levels were found to be reduced in tumors from colorectal cancer patients compared to the adjacent normal tissue, suggesting a plausible link between TIP60 downregulation and tumor progression (14). Colorectal cancer is characterized by inflammation. As such, inflammatory bowel syndrome greatly increases the risk of colorectal cancer (43), highlighting the significance of tumor promoting inflammation in early stages of this cancer. Therefore, we questioned if TIP60 plays a role in the inflammation associated with colorectal cancer. Colorectal cancer cell lines, HCT116 were transiently depleted of TIP60 using siRNA and the cells were harvested 72 h post-transfection. In order to characterize the innate immune response upon TIP60 depletion in greater detail, we studied specific gene expression using real time PCR of the various members of the Interferon Regulatory Factors (IRFs) family, the key transcription factors in mediating the innate immune response (44). Depletion of TIP60 increased the expression of *IRF7* significantly, suggesting a specific role for this transcription factor in mediating the effect of TIP60 (Figure 1A, B and Supplementary Figure S16A). HCT116 cell lines that have stable depletion of TIP60 using shRNA also show increased *IRF7* expression (Supplementary Figure S1A, B and Supplementary Figure S17A). To verify if this increase in IRF7 also occurs in other colorectal cancer cell lines and thus not cell line-specific, we transiently depleted TIP60 in SW620, HT-29 and SW480 cells. Depletion of TIP60 results in an increase in *IRF7* expression at both mRNA (Supplementary Figure S2A–C) and protein levels (Supplementary Figure S2D–F and Supplementary Figure S17B–D). To characterize if this increase is specific to TIP60, we generated a stable cell line that overexpresses wild-type TIP60 (HCT116*TIP60) but is resistant to siRNA. The stable cell lines were validated by performing transient knockdown of TIP60 using two siRNAs: siTIP60A, which could not deplete the exogenous TIP60 (45); and siTIP60B, which efficiently depletes both endogenous and exogenous TIP60 (Figure 1C–E). In order to ascertain that siTIP60A could deplete endogenous TIP60, we designed PCR primers that amplify the 3′UTR of TIP60 which is not present in the exogenous form (expresses only ORF) (Supplementary Figure S3). We observed that both siTIP60A and siTIP60B could efficiently deplete endogenous TIP60 (Figure 1C). Having successfully generated the stable cell line, we proceeded to check the expression of *IRF7*. Depletion of TIP60 using siTIP60A had no effect on *IRF7* expression at either RNA or protein level, but the depletion of TIP60 using siTIP60B showed a robust increase in *IRF7* expression (Figure 1D and E). This suggests that the *IRF7* increase is specific to TIP60. To further investigate whether TIP60-mediated regulation of *IRF7* is conserved across other cancer types, we transiently depleted TIP60 in cervical cancer cells, C33A, as well as in immortalized non-tumorigenic breast epithelial cells, MCF10A and observed an increase in *IRF7* expression (Supplementary Figure S4A–C). This is suggestive of a conserved mechanism of action of TIP60 in cell lines of different cancer origin.

TIP60-mediated IRF7 induction involves bromodomain-containing protein 4 (BRD4)

Acetylated lysine marks on the histones, catalyzed by acetyltransferases such as TIP60 are read by readers like bromodomain-containing protein 4 (BRD4), which recruit other complexes to either activate or repress gene expression (10,46,47). To determine if bromodomain-containing proteins are involved in the TIP60-mediated increase of *IRF7*, we transiently depleted *BRD2*, *BRD3* and *BRD4* in HCT116 cells using siRNA and cells were harvested 72 h post-transfection. We observed an increase in *IRF7* expression upon BRD4 knockdown (Figure 1F and G), similar to that observed upon TIP60 depletion. In contrast, transient depletion of *BRD2* and *BRD3* using siRNAs resulted in no significant induction of *IRF7* (Figure 1F), suggesting the specific involvement of *BRD4*.

By inhibiting the interaction between the reader and the epigenetic mark, gene expression patterns can be altered with JQ1, a chemical inhibitor of BRD4, identified in the context of MYC-driven tumors (48,49). JQ1 acts as a competitive inhibitor of bromodomain-containing proteins, with higher affinity to BRD4. We sought to test the effect of JQ1 treatment on *IRF7* expression. Treatment with 125 nM of JQ1 for 4 h induced *IRF7* expression in HCT116 cells (Figure 1H and I). Different concentrations and time of treatment with JQ1 were performed before identifying the conditions used in this study (Supplementary Figure S5A–C). As with TIP60 depletion, there was no significant change in the other members of IRF family albeit a slight increase in *IRF6* expression (Figure 1H). To ascertain that JQ1-induced *IRF7* increase was not cell line-specific, colorectal cancer cell lines SW480, SW620 and HT-29 were also treated with JQ1 for 4 h and expression of *IRF7* tested. Upon JQ1 treatment, *IRF7* expression increased in all three cell lines (Supplementary Figure S2G–L), similar to HCT116, suggesting a conserved mechanism in colorectal cancer cells. Another group of small molecule inhibitors of BRD4 are the iBET compounds, which are potent and specific inhibitors of the bromodomains of the BRD family (48). Similar to JQ1, I-BET 151 and I-BET 762 have also shown anti-tumor activity in pre-clinical studies (50). I-BET 762 is one of the BET family bromodomain inhibitors which is currently in early Phase I clinical trials (51,52). On treatment of HCT116 cells with 5 μM of I-BET 762 for 4 h, we observed a significant induction of *IRF7* expression (Supplementary Figure S6), similar to observations on TIP60 depletion or treatment with JQ1. These findings further support the involvement of BRD4 in *IRF7* induction.

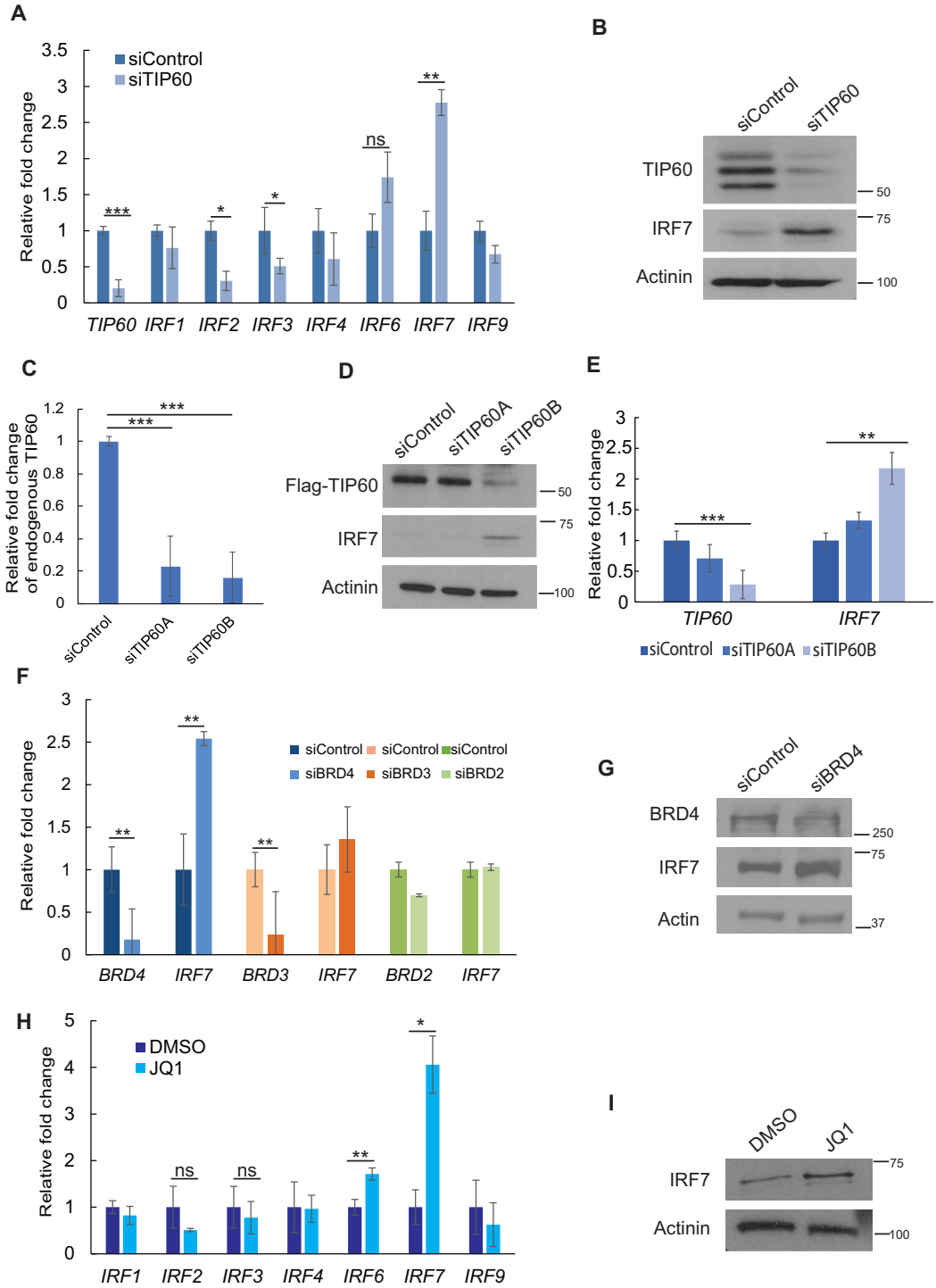

Figure 1. Depletion of TIP60 or BRD4 results in an induction of *IRF7* expression in HCT116 colorectal cancer cell line. (**A**) Depletion of TIP60 in HCT116 colorectal cancer cells using siRNA. Cells were harvested after 72 h and expression of IRF family members was observed. All values are plotted as fold change against *GAPDH*. (**B**) TIP60-depleted cells were harvested and protein lysates resolved using 8% polyacrylamide gel and probed for expression of TIP60 and IRF7 using antibodies to detect endogenous protein levels. (**C**) Detection of endogenous levels of TIP60 by qPCR using specific primers to observe an efficient depletion of TIP60 in siRNA-resistant TIP60-overexpressing HCT116 cells (HCT116-TIP60*WT). (**D**, **E**) Depletion of TIP60 using two different siRNA in HCT116-TIP60*WT cells and monitoring of IRF7 expression at mRNA and protein level using 8 % polyacrylamide gel respectively after 72 h of transfection. Actinin was used as a loading control for all the western blots. (**F**) Depletion of the various members of bromodomain-containing family members, *BRD2*, *BRD3* and *BRD4* using siRNA and monitoring of *IRF7* expression. (**G**) BRD4 is depleted with siRNA and the cells harvested 72 h post transfection, protein lysates obtained and IRF7 expression analyzed using western blot using 8% polyacrylamide gel. Actin serves as the loading control. (**H**, **I**) HCT116 cells were treated with 125 nM of JQ1 for 4 h, cells were harvested and analyzed for mRNA and protein expression of IRF7. Protein samples were resolved on 8% polyacrylamide gels. Error bars represent standard error of mean for at least three independent experiments. ***$P < 0.001$, **$P < 0.01$, *$P < 0.05$.

IRF7 induced by TIP60 activates Type 1 Interferon Response

IRF7 is not constitutively expressed in most immune cells, and is induced upon stimulation of the innate immune response, showing its tight regulation. Hence the upregulation of *IRF7* observed upon TIP60 depletion and JQ1 treatment was intriguing, and indicates the activation of the innate immune signaling pathways in these cells. To verify if the *IRF7* induced is functional, we studied expression of known downstream targets of *IRF7*. We observed a significant increase in the expression of *IFNβ1*, *IFNα1, IFNα4* and *TNFα* in HCT116 cells both under conditions of TIP60 depletion as well as upon JQ1 treatment (Figure 2A–D). To establish that the type 1 interferon response activated upon JQ1 treatment is specific to IRF7, we depleted HCT116 cells of IRF7 transiently and then treated them with JQ1. Upon IRF7 depletion, the induction of *IFNβ1* and *IFNα1* was stunted, highlighting the nodal role played by IRF7 in this response (Figure 2E and F). This suggests that the IRF7 produced is capable of nuclear translocation and inducing the expression of the interferon stimulated genes (ISGs) in these cells.

Reactivation of endogenous retroviral elements activates innate immune signaling cascade in TIP60-depleted cells

The observation of an interferon response upon TIP60 depletion and JQ1 treatment led us to question the origin and stimulus for this response. It is known that the appearance of dsRNA or DNA in the cytoplasm during infection or tissue damage serves to elicit an immune response (53). A potential source of nucleic acids in the cell could be replication intermediates of transposon elements. This hypothesis is also supported by papers which described a 'viral-mimicry' state induced by DNA methylation inhibitors, which leads to demethylation and expression of endogenous retroviral (ERV) elements in tumor cells (29,30). This activates the dsRNA sensing pathways, which invoke an anti-proliferative response in colorectal cancer and also sensitize melanoma cells to anti-CTLA4 immunotherapy (29,30). To study if any of the known retrotransposon elements were regulated upon TIP60 depletion, we performed RNA-seq of siControl and siTIP60-treated HCT116 cells for biological duplicates. We found a significant number of genes that were differentially expressed between siControl and siTIP60 (Supplementary Figure S7, Supplementary Table S4). The data was also analyzed using the RepEnrich software. Of all the groups of repetitive elements that changed upon TIP60 depletion (Figure 3A), the only groups of the elements that increased in expression were those belonging to the class of transposons, more significantly long terminal repeat (LTR) containing transposons. We also identified transposons belonging to different families such ERV L, ERV K and ERV1 to be specifically upregulated upon depletion of TIP60 (Figure 3B). Upon a closer look, we observed different elements within these families of transposons to be upregulated upon TIP60 depletion (Supplementary Figure S8A). Similar analysis was also performed on JQ1 treated samples compared to DMSO vehicle control and we observed a specific increase in LTR class of retrotransposons (Supplementary Figure S8B). In order to validate the RNA-seq as well as to investigate if any of these specific retroviral elements were induced in our system upon TIP60 depletion and/or JQ1 treatment, we screened a few retrotransposon elements by qPCR. We observed an increased in specific ERV elements such as *MER21C, MLT2B4, ERVL, MER4D* and *HERV W* upon both TIP60 depletion and JQ1 treatment (Figure 3C and D), suggesting that the *IRF7* increase could be mounted by the sensing of these ERV RNA/DNA.

TIP60 depletion triggers an interferon response through cytosolic DNA adaptor STING

It is known that IRF7 is specifically upregulated in response to signals from TLR7/8/9 on the endosomal membrane which recognize ssRNA, short dsRNA or CpG containing DNA or through cytosolic RNA (c-RNA) recognition sensors RIG-I and MDA5 (36). A lesser known mechanism of induction of IRF7 is mediated by STING (*TMEM173*), a molecule essential for the innate immune response to c-DNA (54,55). To identify the PRR that leads to increased *IRF7* expression, we transiently depleted HCT116 cells of MAVS, MDA5, RIG-I (involved in c-RNA sensing pathway), or STING (involved in c-DNA sensing pathway) (33) and treated them with JQ1. Depletion of the RNA sensors RIG-I and MDA-5 or the adaptor protein MAVS in this pathway did not abrogate the *IRF7* induction observed upon JQ1 treatment (Supplementary Figure S9A–C). We observed that only depletion of STING resulted in the decrease in *IRF7* response upon treatment with JQ1, suggesting that STING could be involved in the activation of *IRF7* (Figure 4A and Supplementary Figure S9D). Depletion of both TIP60 and STING also resulted in a rescue of IRF7 expression to control level, suggesting that STING plays an important role in the TIP60-mediated *IRF7* increase (Figure 4B, Supplementary Figure S9E and Supplementary Figure S16B). The involvement of STING suggests the presence of c-DNA as a stimulus for the induction of IRF7 (35). In order to test this hypothesis of c-DNA produced by reverse transcription of ERVs upon TIP60 depletion or JQ1 treatment, we treated HCT116 cells with a combination of known reverse transcriptase (RT) inhibitors, Zidovudine (Azt) and Nevirapine (Nev) for 48 h. Four hours prior to harvest, these cells were treated with JQ1 and IRF7 induction was monitored. We observed a rescue of IRF7 expression to control level upon treatment with RT inhibitors (Figure 4C), and a similar observation upon TIP60 depletion followed by treatment with RT inhibitors (Figure 4D and Supplementary Figure S16C). Since there was a rescue of IRF7 expression on treatment with RT inhibitors, we investigated if TIP60 confers any resistance to RT inhibitors treatment. In both MTT assay as well as long term proliferation assay, TIP60-depleted cells show a higher sensitivity to treatment with combination of RT inhibitors as compared to siControl-treated cells (Figure 4E–H, Supplementary Figures S10 and S11), suggesting the importance and dependence of tumor cells on the aberrantly transcribed ERVs under low levels of TIP60. Similar observation of sensitivity to RT inhibitor combination was also observed in HCT116 cells stably depleted of TIP60 using shRNA (Supplementary Figure S1C and D).

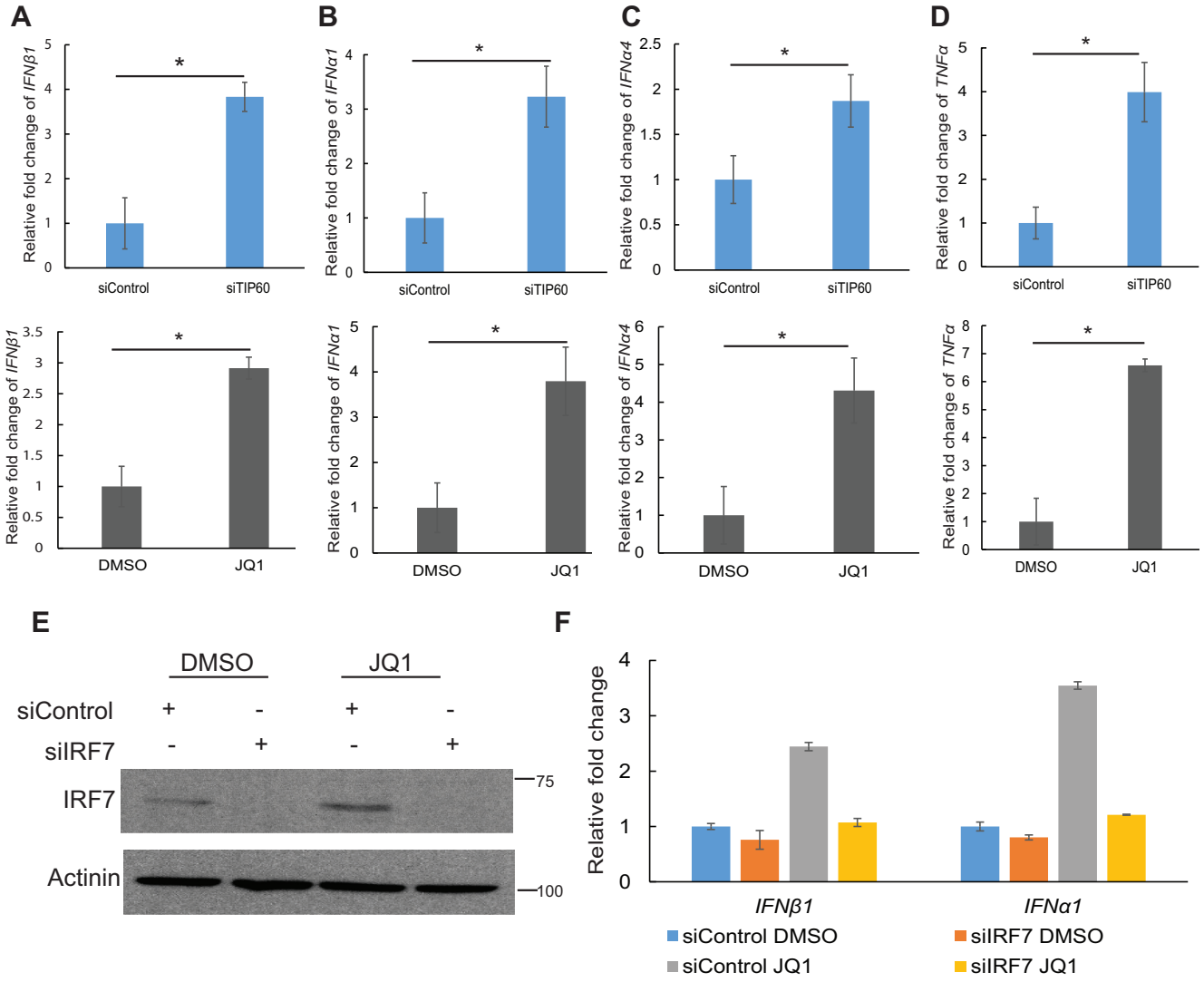

Figure 2. Depletion of TIP60 and JQ1 treatment activate an IRF7-dependent type-1 interferon response. (**A–D**) Depletion of TIP60 by siRNA or treatment with 125 nM JQ1 for 4 h resulted in increase of expression of type-1 interferons *IFNβ1*, *IFNα1*, *IFNα4* and *TNFα* respectively. (**E**, **F**) Transient depletion of *IRF7* by siRNA and treatment with 125 nM JQ1 for 4 h prior to harvesting cells to monitor expression of *IFNβ1* and *IFNα1*, the downstream targets of IRF7. Protein samples were resolved on 8% polyacrylamide gels. Error bars represent standard error of mean for three independent experiments. $*P < 0.05$.

TIP60 positively regulates expression of histone methyltransferases (HMTs)

Endogenous retroviruses are known to be silenced cooperatively by multiple factors including KAP1, a corepressor protein, and H3K9 methyltransferases SETDB1 and SUV39H1 (22,23,56,57). The promoters of these retroviral elements are selectively enriched in Histone variant H3.3 as well as the histone mark H3K9me3, which are essential in maintaining the repressed state of these repetitive elements (22,56). We hypothesized that TIP60 could regulate the expression of one or more of these factors, thereby affecting global transposon expression in tumor cells. We observed a global decrease in H3K9me3 upon depletion of TIP60 (Figure 5A and Supplementary Figure S16D), a known repressive mark at the LTRs of transposons, suggesting a misregulation in the expression of histone methylating enzymes. Indeed, upon revisiting our RNA-seq data from HCT116 siControl and siTIP60-treated samples, we observed a significant decrease in expression of these H3K9 trimethylating enzymes - *SUV39H1* and *SETDB1* in TIP60-depleted cells (Supplementary Figure S7). This was also verified by qPCR (Figure 5B). Interestingly, treatment with JQ1 also resulted in a decrease in the expression of these enzymes (Figure 5C). The global decrease in H3K9me3, could serve to explain the genome-wide increase in transposon expression on depletion of TIP60. To test if this was the case, we depleted SUV39H1 and SETDB1 using siRNA individually and observed an increase in the expression of IRF7 and ERVs consistent with our previous observations upon TIP60 depletion (Supplementary Figure S12A–E). Interestingly, upon treatment of the SETDB1 or SUV39H1-depleted cells with RT inhibitors, we observed that SETDB1-depleted cells and cells depleted of both

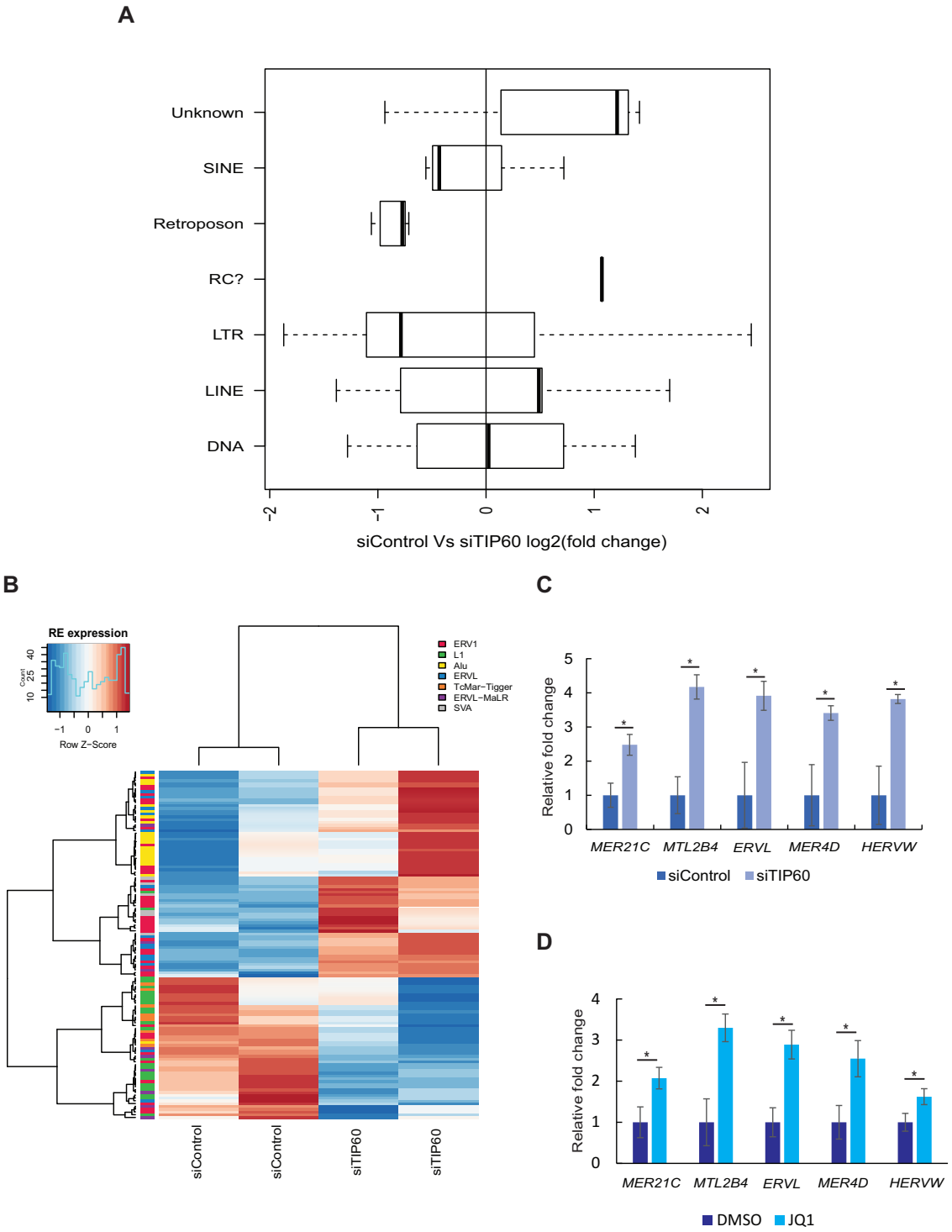

Figure 3. Differential expression of transposable elements after depletion of TIP60 and JQ1 treatment. HCT116 cells were transiently depleted of TIP60 using siRNA and the RNA isolated for 2 biological replicates was sent for sequencing. The results were analyzed using RepEnrich software. (**A**) Box plots showing the expression differences for control and TIP60-depleted conditions for different transposon classes. Differences in expression are shown as the log 2-fold change between control and TIP60-knockdown conditions (positive values represent higher expression levels in control condition while negative values show higher expression in the knockdown). Only transposable elements with significant differences (FDR 5%) were used for this analysis. Unknown annotation according to repeat masker is the default when the class of transposable elements is missing or unknown. RC refers to rolling circle. Retroposons also belong to LTR family but may not encode a function reverse transcriptase. DNA refers to DNA repeat elements. (**B**) Heat map showing the RNA-seq signal enrichment in repetitive elements with an FDR lower than 5%. Elements and samples are arranged based on the results of hierarchical clustering and the classes they belong to are shown as a color label on row side panel. (**C**, **D**) qPCR validation of selected retrotransposon elements after depletion of TIP60 and JQ1 treatment respectively. mRNA fold changes are normalized to *GAPDH*. Error bars represent standard error of mean for three independent experiments. *, $P<0.05$.

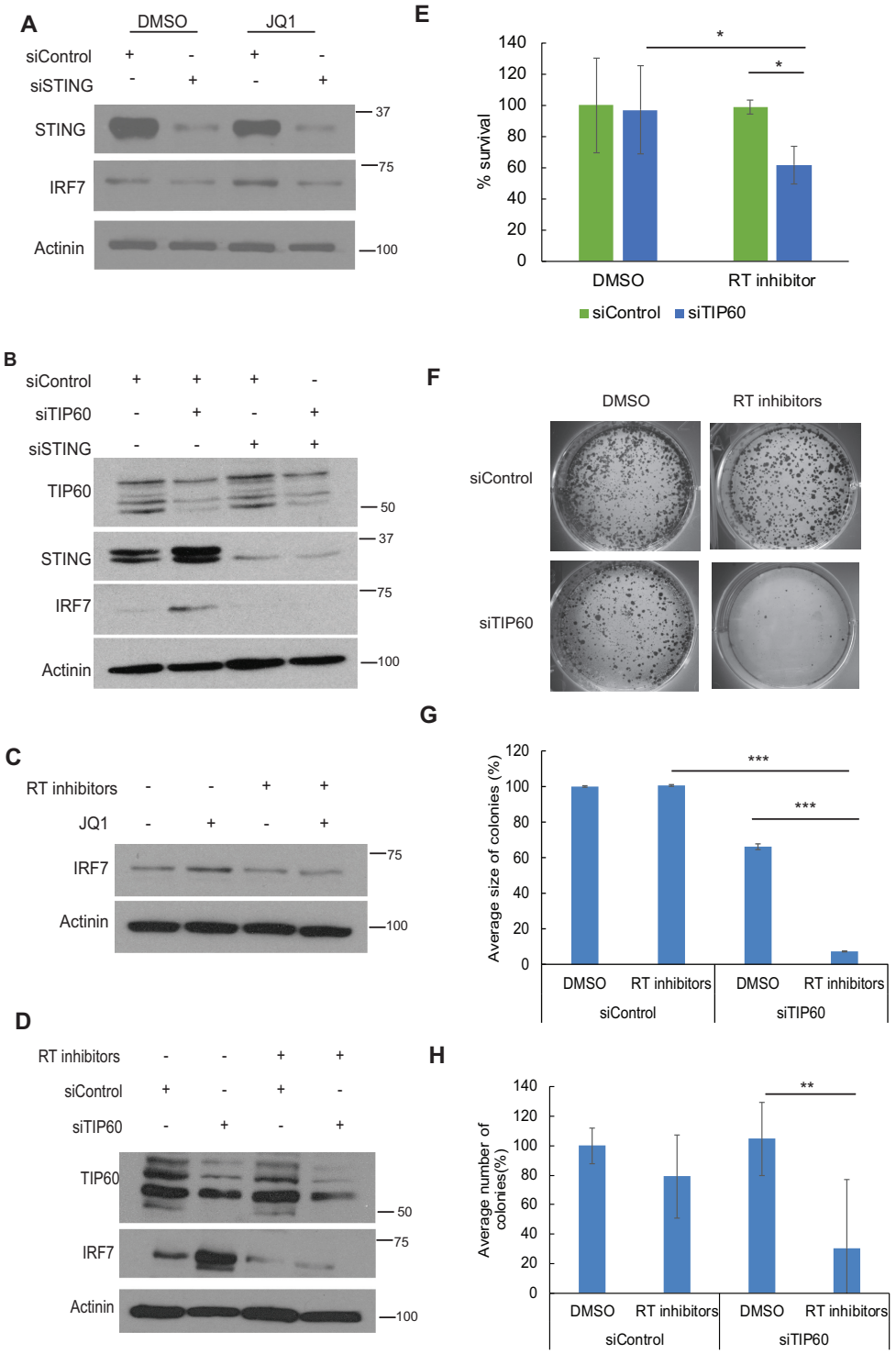

Figure 4. TIP60 induces IRF7 expression through cytosolic DNA sensing by STING. (**A**) Transient knockdown of STING using siRNA and treatment with JQ1 for 4 h prior to harvesting and western blot analysis using 8% polyacrylamide gel to study IRF7 expression. (**B**) Co-depletion of STING and TIP60 using siRNA in HCT116 cells and western blot from samples run on 8% polyacrylamide gel to detect IRF7 expression. (**C**) Treatment of HCT116 cells with 20 μM each of Zidovudine and Nevirapine for 48 h. Cells were either treated with DMSO or JQ1 4 h prior to harvesting and western blot analysis using 8% polyacrylamide gel for IRF7 expression. (**D**) Treatment of HCT116 cells with 20 μM each of Zidovudine and Nevirapine for 48 h after TIP60 depletion by siRNA. Cells were harvested 72 h after knockdown and IRF7 expression was analyzed using 8% polyacrylamide gel. Actinin was used as loading control. (**E**, **F**) TIP60 was transiently depleted using siRNA. Twenty-four hours after transfection, 1×10^4 HCT116 cells per well in a 96-well plate were seeded in triplicates for MTT assay and 2000 cells for colony formation assay (CFA) either in the presence or absence of RT inhibitors (20 μM each of Nevirapine and Zidovudine). The cell survival was assayed 48 h after treatment with RT inhibitors. For CFA, Cells were stained 11 days after seeding and quantified using Image J software. (F) Representative image of the colonies obtained on staining. Quantification of the average size (**G**) and number (**H**) of colonies using Image J. Error bars reflect SEM for three independent experiments. $^{***}P < 0.001$, $^{**}P < 0.01$, $^{*}P < 0.05$.

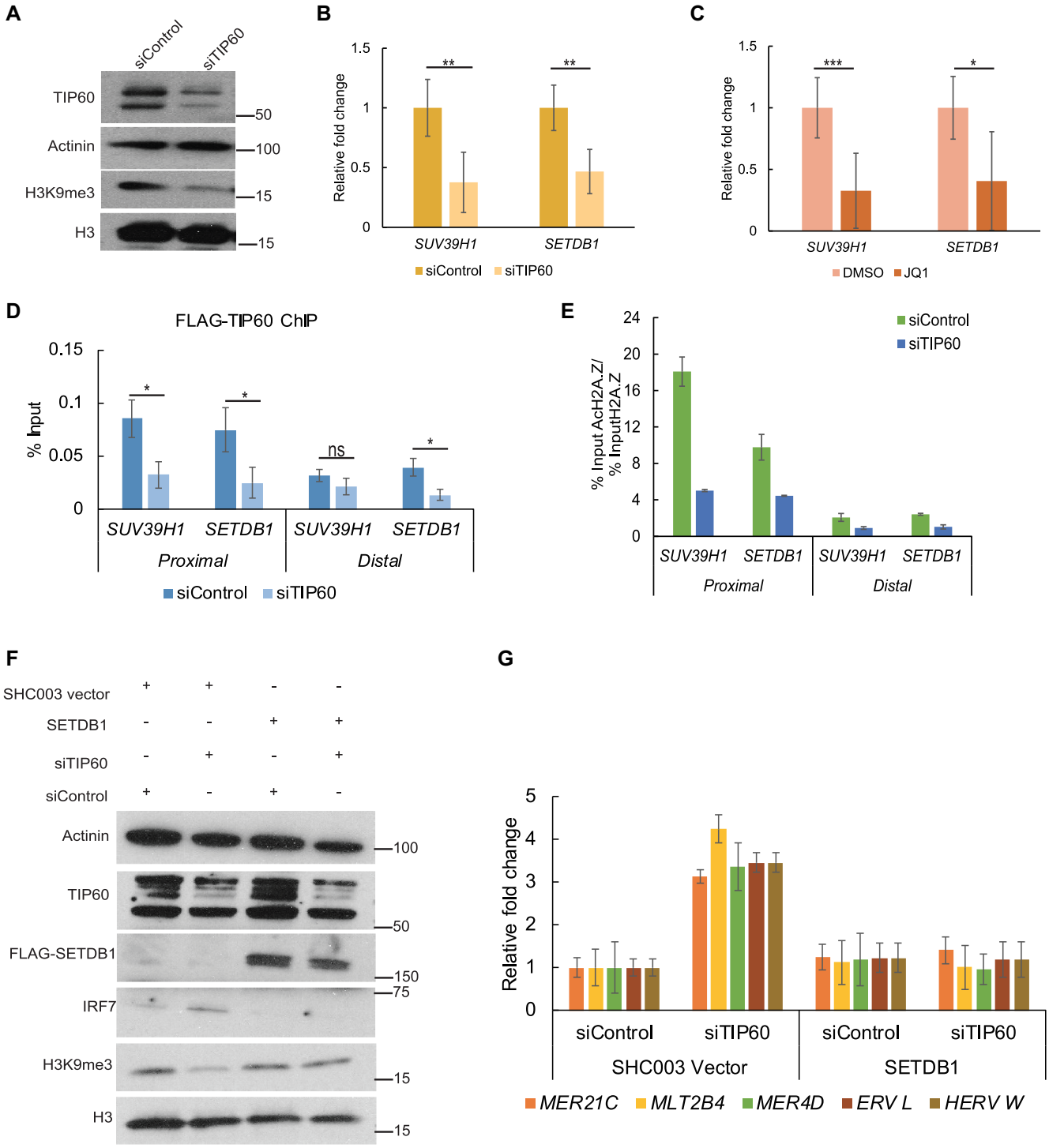

Figure 5. TIP60 is a positive regulator of HMTs. (**A**) Depletion of TIP60 by siRNA and western blot analysis using antibodies for endogenous TIP60, H3K9me3 and H3 using a 4–15% precast gradient polyacrylamide gel. (**B, C**) Detection of expression of *SUV39H1* and *SETDB1* by qPCR after depletion of TIP60 and treatment with JQ1 respectively. (**D**) Chromatin immunoprecipitation (ChIP) assay performed with anti-FLAG antibody and (**E**) Representative ChIP for anti-acetyl H2A.Z normalized to H2A.Z, in HCT116-TIP60WT cells. For the histone ChIP, error bars represent SEM of technical replicates. Regions proximal to TSS show enrichment of signal compared to the distal regions. (**F**) SETDB1 was transiently overexpressed in HCT116 cells. Twenty-four hours post plasmid transfection, the cells were transiently depleted of TIP60 using siRNA. Cells were harvested 48 h later and lysates were processed for western blotting using 4–15% precast gradient polyacrylamide gels. (**G**) qPCR for ERVs following overexpression of SETDB1 and TIP60 depletion. Error bars represent SEM for at least three independent biological replicates. $***P < 0.001$, $**P < 0.01$, $*P < 0.05$.

SUV39H1 and SETDB1 were sensitive to RT inhibitors compared to siControl treated cells (Supplementary Figure S12F and G). This similarity in response to RT inhibitors between depletion of SETDB1 and SUV39H1 and depletion of TIP60, reiterates the role of these enzymes in mediating the repression of ERVs by TIP60. We next sought to identify how TIP60 regulates the expression of these HMTs. We transiently depleted TIP60 in HCT116-TIP60WT cells, which overexpress FLAG-tagged TIP60 and observed a similar decrease in expression of *SUV39H1* and *SETDB1* (Supplementary Figure S13A). We then performed ChIP with anti-FLAG antibody to detect if TIP60 is enriched at the promoters of these genes. We detected a specific enrichment of FLAG-tagged TIP60 at the TSS of these HMTs and a few other genes identified in our RNA-seq data (Figure 5D, Supplementary Figure S13B and C). BRD4 is also enriched in a TIP60 dependent manner at the proximal regions of *SUV39H1* and *SETDB1* (Supplementary Figure S13D). The specificity of BRD4 ChIP was confirmed by performing the same experiment under conditions of BRD4 depletion (Supplementary Figure S13E). We also performed ChIP for acetylated H2A.Z (AcH2A.Z), a mark associated with actively transcribed regions and a newly identified histone substrate of TIP60 (Zhang *et al*. unpublished). Interestingly, we observe a TIP60 specific enrichment of AcH2A.Z, a mark known to be associated with active chromatin, at the promoters of *SUV39H1*and *SETDB1* (Figure 5E).

To establish the critical role played by SETDB1 and SUV39H1 in TIP60-mediated ERV repression, we questioned if overexpression of either of these two HMTs could rescue the IRF7 increase and ERV de-repression observed upon TIP60 depletion. We transiently transfected plasmids for overexpression FLAG-tagged SETDB1 (pLKO-SETDB1) (37) or SUV39H1 (LPCX-SUV39H1) into HCT116 cells. Twenty-four hours after plasmid transfection, we performed transient depletion of TIP60 using siRNA. Forty-eight hours later, the cells were harvested and analyzed for protein and mRNA expression. We observe that overexpression of either SUV39H1 or SETDB1 can indeed rescue the increase in IRF7 expression upon TIP60 depletion to control levels as well as restore the global H3K9me3 levels (Figure 5F, Supplementary Figures S14A, S16E and S17E). Depletion of TIP60 results in an increase in ERV transcription, consistent with our previous findings. Overexpression of SETDB1 is sufficient to repress the ERV induction upon TIP60 depletion. This suggests that TIP60 represses ERVs through SETDB1 (Figure 5G). We do observe a marginal reduction even in SETDB1 overexpression upon TIP60 depletion, suggesting that there could be an additional layer of post-transcriptional regulation, which remains to be studied. Although, we do not see changes in ERV expression pattern upon SUV39H1 overexpression (Supplementary Figure S14B), we do see a rescue in both IRF7 expression and H3K9me3 level, suggesting it could also play a role in TIP60-mediated global repression of ERVs. It has been documented in mouse models that SETDB1 and SUV39H1 target distinct groups of transposons for repression and we speculate this could be conserved in humans as well (23,57).

Restoration of TIP60 represses ERVs and inhibits tumor growth

HCT116 cells which stably overexpress wild-type TIP60 were generated. Stable overexpression of TIP60 in HCT116 cells resulted in the repression of these ERV elements, implicating the role of TIP60 in the stable silencing of ERVs (Figure 6A, B and Supplementary Figure S16F). In order to study if TIP60 overexpression could impede the growth of these tumorigenic cells, we performed colony formation assay. We observed a decrease in the growth of cells overexpressing TIP60, highlighting the tumor suppressive role of TIP60 in colorectal cancer (Figure 6C and D). We were curious to know if a similar phenotype could be observed in an *in vivo* system and hence subcutaneously injected NOD/SCID mice with one million cells of HCT116-MSCV and HCT116-TIP60 in the left and right flank respectively. The tumors were allowed to grow and the volume was measured at 7-day intervals until the end of the experiment at 21 days. We observed a significant reduction in growth upon overexpression of TIP60 in this model in the mice. The mice where the tumors grow more than 150 mm^3 in volume in the HCT116-MSCV were used to calculate the differences in tumor size and we observed a significant decrease in tumor size at day 21 in tumors that overexpress TIP60 compared to MSCV vector injected tumors (Figure 6E). We wanted to test if the tumors which show a reduced size upon TIP60 overexpression (Figure 6F and G) do indeed express TIP60. For this, the tumors were lysed and analyzed by western blot. We could detect expression of FLAG-tagged TIP60 in HCT116-TIP60 injected tumors and not in the HCT116-MSCV injected tumors (Figure 6H). This data shows that overexpression of TIP60 reduces tumorigenic ability *in vitro* and *in vivo* and that reactivation of ERVs could provide growth advantage to tumorigenic cells (Figure 7).

DISCUSSION

Genomic instability and mutation as well as tumor promoting inflammation are now recognized as two of the enabling characteristics of tumorigenesis (58). The knowledge of their regulation and their source in the tumor cells are largely unexplored. We have identified TIP60, a tumor suppressor, to be involved in suppressing both enabling characteristics, thereby providing a mechanistic reason for the widespread downregulation of TIP60 in different types of tumors.

An increasing body of evidence highlights the link between chronic inflammation and tumorigenesis. Bacterial or viral infection-mediated inflammatory processes can potentially accelerate tumorigenesis, as suggested by the strong association between Crohn's disease or chronic ulcerative colitis and colorectal cancer (43); *Helicobacter pylori* infection and gastric cancer (59); human papillomavirus infection and cervical cancer; Hepatitis B and C virus infection and liver cancer; and chronic bronchitis and lung cancer (60,61). Toll-like receptors (TLRs) play an important role in the innate immune system as responders to invading pathogens. Activation of TLRs by their specific ligands activate the signaling cascade downstream, which leads to transcription of Interferon Regulatory Factors (IRFs) and

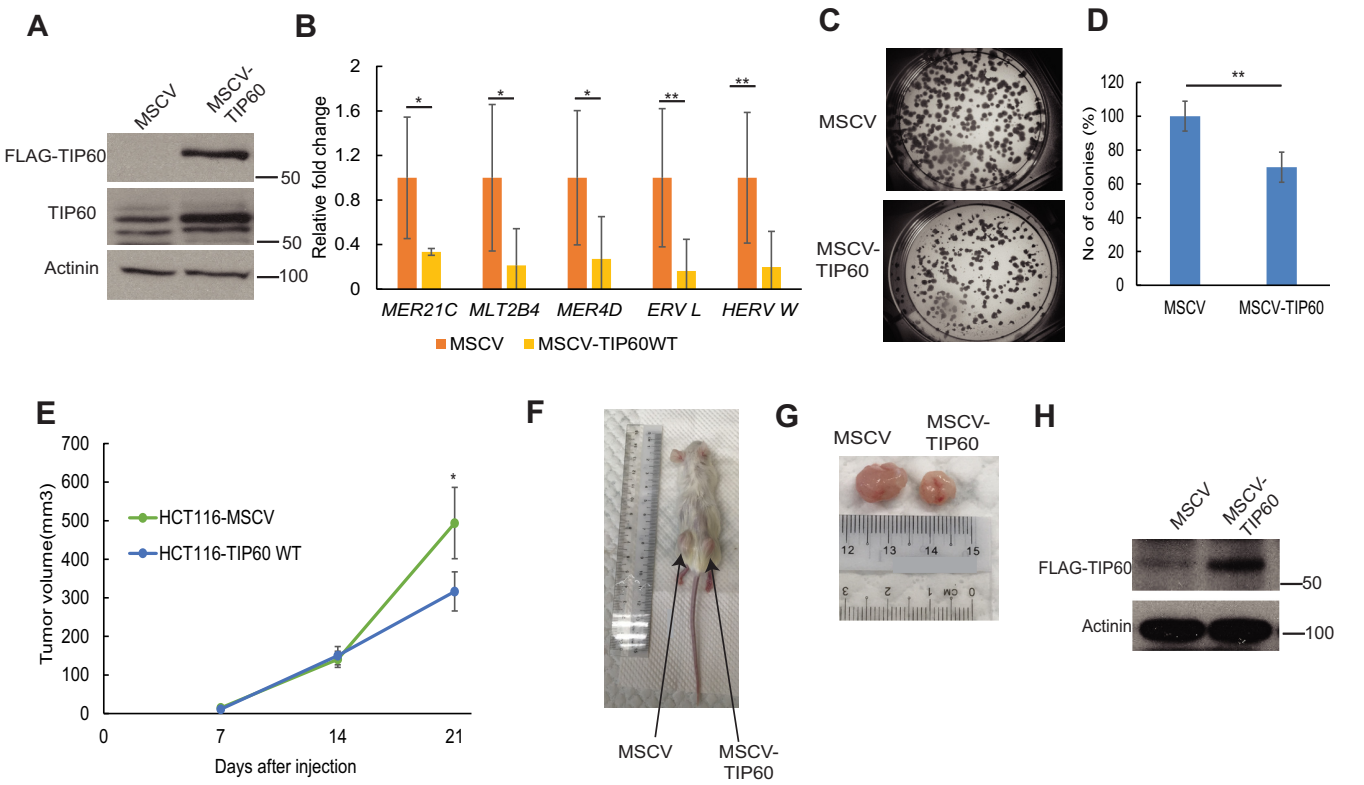

Figure 6. Overexpression of TIP60 represses ERVs and inhibits tumor growth. (**A**, **B**) Expression of ERVs and TIP60 in HCT116 cells overexpressing wild-type TIP60 using qPCR and 8% polyacrylamide gel to check protein expression. (**C**, **D**) Fifteen hundred cells were seeded for colony formation. Colonies were fixed with 20% methanol and stained with crystal violet, 11 days after seeding. Quantification of number of colonies performed using Image J software. Error bars represent standard error of mean of at least three independent experiments., $^{**}P < 0.01$, $^{*}P < 0.05$. (**E**) Tumor growth monitored in 12 mice over a period of 21 days. (**F**) Representative image of mouse injected subcutaneously with HCT116-MSCV on the left flank and HCT116-TIP60 on the right flank. (**G**) Image showing difference in tumor size between HCT116-MSCV and HCT116-TIP60 cells. (**H**) Harvested tumors were tested for expression of Flag-tagged TIP60.

induction of an inflammatory response (34,44). Many cancers of epithelial origin have been identified to possess these TLRs, indicating a potential tumor supportive function (62,63). For instance, activation of signaling through TLR9 in prostate cancer increases their metastatic ability and the expression of TLR9 is correlated with poor prognosis (64,65). TIP60 depletion leads to an increase in inflammatory response in cancer cells (Figure 1), thereby providing a molecular mechanism for TIP60 as a tumor suppressor. Since the level of TIP60 protein could be different across the different cancer cell lines, even small changes in TIP60 level could still result in induction of IRF7 expression as we observe in the case of SW620 and HT-29 cells.

Depletion of TIP60 in colorectal cancer cells is also associated with a genome-wide de-repression of ERVs (Figure 3). JQ1 treatment and BRD4 depletion also mimic TIP60 depletion, suggesting that BRD4 could be 'reading' the acetyl marks put by TIP60 on chromatin. Although we show regulation of HMTs to be critical in mediating TIP60's repressive effect on ERVs, it could also be possible that in addition, TIP60 could recognize and be recruited to the promoter/LTR sequences of transposon elements genome-wide and thus regulate their expression at two levels.

TIP60 is known to be recruited to chromatin through its chromo-domain, which upon recognition of H3K9me3 brings TIP60 to chromatin and activates its acetyltransferase activity (66). Identifying TIP60 to regulate global H3K9me3 levels, adds an interesting feedforward regulation to this dynamic interaction. Intriguingly, promoters of endogenous retroviral elements are marked by enrichment of H3K9me3 (22,23), leading us to hypothesize that TIP60 could be selectively recruited to these promoters by this histone mark and may have a role to play here. As a preliminary study, we performed ChIP for FLAG-tagged TIP60 and looked for its occupancy at potential LTR regions of the ERVs where we observe changes in expression upon TIP60 depletion. We do see an enriched occupancy of TIP60 at a few potential LTRs (Supplementary Figure S15), which needs to be further investigated to understand if TIP60 has a role to play at LTRs. Endogenous retroviruses are known to be silenced cooperatively by multiple factors (22–24,57). Although we observe that overexpression of SUV39H1 is sufficient to ablate the IRF7 induction upon TIP60 depletion, the ERVs tested by qPCR still show increased transcription. This suggests that SUV39H1 may regulate a separate category of transposons upon TIP60 depletion, whose reactivation also contributes to IRF7 induction. Alternatively, SUV39H1 could also regulate any of the intermediary steps in reverse transcription of ERVs, detection of c-

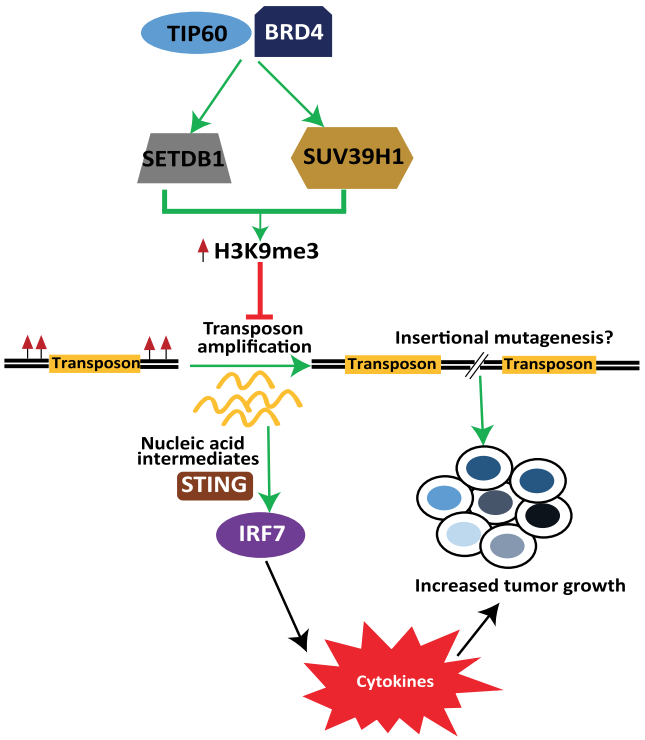

Figure 7. TIP60-mediated ERV repression in colorectal cancer. Schematic representation of the dynamic interaction between TIP60 and BRD4 to silence transposons failing which leads to the activation of STING-mediated IRF7 increase and type 1 interferon production.

DNA and signaling through STING, resulting in increased IRF7. These remain interesting directions for future studies.

The sensitivity observed upon TIP60 depletion to RT inhibitors has immense therapeutic potential. Colorectal tumors with low TIP60 can be analyzed for the expression of retroviral elements signature and can be treated with RT inhibitor drugs to effectively modulate the tumor growth and tumor immune response.

In conclusion, this study has identified a previously uncharacterized tumor suppressive function of TIP60 which involves repression of endogenous retroviral elements in colorectal cancer cells by reducing global H3K9me3 through reduction of expression of SUV39H1, and SETDB1 (Figure 7). Downregulation of TIP60 in different tumors results in re-activation of these elements, which are detected by the cellular innate immune system and trigger an interferon response. The induction of *IRF7* further activates the type I interferon response production of inflammatory cytokines and chemokines.

SUPPLEMENTARY DATA

Supplementary Data are available at NAR Online.

ACKNOWLEDGEMENTS

We thank the members of the Jha laboratory for helpful discussion and comments.

Author Contributions: D.R. and S.J. designed and conceived the experiments used in this study. D.R. conducted the experiments. SSB performed replicates of ChIP-seq for H3K9me3. S.S. did the library preparation, size selection and sequencing of one biological replicate for ChIP. S.H. performed a few long-term growth assays and a replicate of western blot. K.K.L. performed survival assay and helped in cloning of SUV39H1. Y.Z. generated some of the initial ChIP data for AcH2A.Z. W.S.T. conducted the xenograft experiments. S.P.J. tried to generate few of the stable cell lines. R.T.M. and Y.W. conducted and, T.B. and N.K. supervised the bioinformatics analysis used in this study. Y.H.G. helped in the better design of experiments and provided valuable intellectual input.

FUNDING

National Research Foundation Singapore and the Singapore Ministry of Education under its Research Centers of Excellence initiative to the Cancer Science Institute of Singapore [R-713-006-014-271 to S.J.]; National Medical Research Council [NMRC CBRG-NIG BNIG11nov001 to S.J.]; Ministry of Education Academic Research Fund [MOE AcRF Tier 1 T1-2012 Oct-04 and T1-2016 Apr-01 to S.J.]; RNA Biology Center at CSI Singapore, NUS, from funding by the Singapore Ministry of Education's Tier 3 grants [MOE2014-T3-1-006 to S.J. and T.B.]; Yong Loo Lin School of Medicine, National University of Singapore (to D.R. and S.H.); Cancer Science Institute of Singapore, Yong Loo Lin School of Medicine, National University of Singapore (to R.T.M., S.S.B., K.K.L. and Y.Z.). S.J., T.B. and R.T.M. thank the Merlion Ph.D. programme (funded by the French Ministry for Europe and Foreign Affairs, and the French Ministry for Higher Education, Research and Innovation) for the support provided to R.T.M. Ph.D. studies.

Conflict of interest statement. None declared.

REFERENCES

1. Doyon,Y. and Cote,J. (2004) The highly conserved and multifunctional NuA4 HAT complex. *Curr. Opin. Genet. Dev.*, **14**, 147–154.
2. Avvakumov,N. and Cote,J. (2007) The MYST family of histone acetyltransferases and their intimate links to cancer. *Oncogene*, **26**, 5395–5407.
3. Sun,Y., Jiang,X., Chen,S., Fernandes,N. and Price,B.D. (2005) A role for the Tip60 histone acetyltransferase in the acetylation and activation of ATM. *Proc. Natl. Acad. Sci. U.S.A.*, **102**, 13182–13187.
4. Sykes,S.M., Mellert,H.S., Holbert,M.A., Li,K., Marmorstein,R., Lane,W.S. and McMahon,S.B. (2006) Acetylation of the p53 DNA-binding domain regulates apoptosis induction. *Mol. Cell*, **24**, 841–851.
5. Tang,Y., Luo,J., Zhang,W. and Gu,W. (2006) Tip60-dependent acetylation of p53 modulates the decision between cell-cycle arrest and apoptosis. *Mol. Cell*, **24**, 827–839.
6. Kimura,A. and Horikoshi,M. (1998) Tip60 acetylates six lysines of a specific class in core histones in vitro. *Genes Cells*, **3**, 789–800.
7. Gaughan,L., Logan,I.R., Cook,S., Neal,D.E. and Robson,C.N. (2002) Tip60 and histone deacetylase 1 regulate androgen receptor activity through changes to the acetylation status of the receptor. *J. Biol. Chem.*, **277**, 25904–25913.
8. Patel,J.H., Du,Y., Ard,P.G., Phillips,C., Carella,B., Chen,C.J., Rakowski,C., Chatterjee,C., Lieberman,P.M., Lane,W.S. *et al.* (2004) The c-MYC oncoprotein is a substrate of the acetyltransferases hGCN5/PCAF and TIP60. *Mol. Cell. Biol.*, **24**, 10826–10834.
9. Frank,S.R., Parisi,T., Taubert,S., Fernandez,P., Fuchs,M., Chan,H.M., Livingston,D.M. and Amati,B. (2003) MYC recruits the

TIP60 histone acetyltransferase complex to chromatin. *EMBO Rep.*, **4**, 575–580.
10. Jha,S., Vande Pol,S., Banerjee,N.S., Dutta,A.B., Chow,L.T. and Dutta,A. (2010) Destabilization of TIP60 by human papillomavirus E6 results in attenuation of TIP60-dependent transcriptional regulation and apoptotic pathway. *Mol. Cell*, **38**, 700–711.
11. Gupta,A., Jha,S., Engel,D.A., Ornelles,D.A. and Dutta,A. (2013) Tip60 degradation by adenovirus relieves transcriptional repression of viral transcriptional activator EIA. *Oncogene*, **32**, 5017–5025.
12. Rajagopalan,D., Pandey,A.K., Xiuzhen,M.C., Lee,K.K., Hora,S., Zhang,Y., Chua,B.H., Kwok,H.S., Bhatia,S.S., Deng,L.W. *et al.* (2017) TIP60 represses telomerase expression by inhibiting Sp1 binding to the TERT promoter. *PLoS Pathog.*, **13**, e1006681.
13. Gorrini,C., Squatrito,M., Luise,C., Syed,N., Perna,D., Wark,L., Martinato,F., Sardella,D., Verrecchia,A., Bennett,S. *et al.* (2007) Tip60 is a haplo-insufficient tumour suppressor required for an oncogene-induced DNA damage response. *Nature*, **448**, 1063–1067.
14. Mattera,L., Escaffit,F., Pillaire,M.J., Selves,J., Tyteca,S., Hoffmann,J.S., Gourraud,P.A., Chevillard-Briet,M., Cazaux,C. and Trouche,D. (2009) The p400/Tip60 ratio is critical for colorectal cancer cell proliferation through DNA damage response pathways. *Oncogene*, **28**, 1506–1517.
15. Subbaiah,V.K., Zhang,Y., Rajagopalan,D., Abdullah,L.N., Yeo-Teh,N.S., Tomaic,V., Banks,L., Myers,M.P., Chow,E.K. and Jha,S. (2016) E3 ligase EDD1/UBR5 is utilized by the HPV E6 oncogene to destabilize tumor suppressor TIP60. *Oncogene*, **35**, 2062–2074.
16. Michor,F., Iwasa,Y. and Nowak,M.A. (2004) Dynamics of cancer progression. *Nat. Rev. Cancer*, **4**, 197–205.
17. Chaffer,C.L. and Weinberg,R.A. (2015) How does multistep tumorigenesis really proceed? *Cancer Discov.*, **5**, 22–24.
18. Lander,E.S., Linton,L.M., Birren,B., Nusbaum,C., Zody,M.C., Baldwin,J., Devon,K., Dewar,K., Doyle,M., FitzHugh,W. *et al.* (2001) Initial sequencing and analysis of the human genome. *Nature*, **409**, 860–921.
19. Mills,R.E., Bennett,E.A., Iskow,R.C. and Devine,S.E. (2007) Which transposable elements are active in the human genome? *Trends Genet.*, **23**, 183–191.
20. Volkman,H.E. and Stetson,D.B. (2014) The enemy within: endogenous retroelements and autoimmune disease. *Nat. Immunol.*, **15**, 415–422.
21. Young,G.R., Mavrommatis,B. and Kassiotis,G. (2014) Microarray analysis reveals global modulation of endogenous retroelement transcription by microbes. *Retrovirology*, **11**, 59.
22. Rowe,H.M., Jakobsson,J., Mesnard,D., Rougemont,J., Reynard,S., Aktas,T., Maillard,P.V., Layard-Liesching,H., Verp,S., Marquis,J. *et al.* (2010) KAP1 controls endogenous retroviruses in embryonic stem cells. *Nature*, **463**, 237–240.
23. Liu,S., Brind'Amour,J., Karimi,M.M., Shirane,K., Bogutz,A., Lefebvre,L., Sasaki,H., Shinkai,Y. and Lorincz,M.C. (2014) Setdb1 is required for germline development and silencing of H3K9me3-marked endogenous retroviruses in primordial germ cells. *Genes Dev.*, **28**, 2041–2055.
24. Matsui,T., Leung,D., Miyashita,H., Maksakova,I.A., Miyachi,H., Kimura,H., Tachibana,M., Lorincz,M.C. and Shinkai,Y. (2010) Proviral silencing in embryonic stem cells requires the histone methyltransferase ESET. *Nature*, **464**, 927–931.
25. Walsh,C.P., Chaillet,J.R. and Bestor,T.H. (1998) Transcription of IAP endogenous retroviruses is constrained by cytosine methylation. *Nat. Genet.*, **20**, 116–117.
26. Okano,M., Bell,D.W., Haber,D.A. and Li,E. (1999) DNA methyltransferases Dnmt3a and Dnmt3b are essential for de novo methylation and mammalian development. *Cell*, **99**, 247–257.
27. Serafino,A., Balestrieri,E., Pierimarchi,P., Matteucci,C., Moroni,G., Oricchio,E., Rasi,G., Mastino,A., Spadafora,C., Garaci,E. *et al.* (2009) The activation of human endogenous retrovirus K (HERV-K) is implicated in melanoma cell malignant transformation. *Exp. Cell Res.*, **315**, 849–862.
28. Bhardwaj,N., Montesion,M., Roy,F. and Coffin,J.M. (2015) Differential expression of HERV-K (HML-2) proviruses in cells and virions of the teratocarcinoma cell line Tera-1. *Viruses*, **7**, 939–968.
29. Chiappinelli,K.B., Strissel,P.L., Desrichard,A., Li,H., Henke,C., Akman,B., Hein,A., Rote,N.S., Cope,L.M., Snyder,A. *et al.* (2015) Inhibiting DNA methylation causes an interferon response in cancer via dsRNA including endogenous retroviruses. *Cell*, **162**, 974–986.
30. Roulois,D., Loo Yau,H., Singhania,R., Wang,Y., Danesh,A., Shen,S.Y., Han,H., Liang,G., Jones,P.A., Pugh,T.J. *et al.* (2015) DNA-Demethylating agents target colorectal cancer cells by inducing viral mimicry by endogenous transcripts. *Cell*, **162**, 961–973.
31. Lee,E., Iskow,R., Yang,L., Gokcumen,O., Haseley,P., Luquette,L.J. 3rd, Lohr,J.G., Harris,C.C., Ding,L., Wilson,R.K. *et al.* (2012) Landscape of somatic retrotransposition in human cancers. *Science*, **337**, 967–971.
32. Kassiotis,G. and Stoye,J.P. (2016) Immune responses to endogenous retroelements: taking the bad with the good. *Nat. Rev. Immunol.*, **16**, 207–219.
33. Akira,S. (2009) Pathogen recognition by innate immunity and its signaling. *Proc. Jpn. Acad. Ser. B Phys. Biol. Sci.*, **85**, 143–156.
34. Akira,S., Uematsu,S. and Takeuchi,O. (2006) Pathogen recognition and innate immunity. *Cell*, **124**, 783–801.
35. Cai,X., Chiu,Y.H. and Chen,Z.J. (2014) The cGAS-cGAMP-STING pathway of cytosolic DNA sensing and signaling. *Mol. Cell*, **54**, 289–296.
36. Honda,K. and Taniguchi,T. (2006) IRFs: master regulators of signalling by Toll-like receptors and cytosolic pattern-recognition receptors. *Nat. Rev. Immunol.*, **6**, 644–658.
37. Sun,Q.Y., Ding,L.W., Xiao,J.F., Chien,W., Lim,S.L., Hattori,N., Goodglick,L., Chia,D., Mah,V., Alavi,M. *et al.* (2015) SETDB1 accelerates tumourigenesis by regulating the WNT signalling pathway. *J. Pathol.*, **235**, 559–570.
38. Jha,S., Shibata,E. and Dutta,A. (2008) Human Rvb1/Tip49 is required for the histone acetyltransferase activity of Tip60/NuA4 and for the downregulation of phosphorylation on H2AX after DNA damage. *Mol. Cell. Biol.*, **28**, 2690–2700.
39. Dobin,A., Davis,C.A., Schlesinger,F., Drenkow,J., Zaleski,C., Jha,S., Batut,P., Chaisson,M. and Gingeras,T.R. (2013) STAR: ultrafast universal RNA-seq aligner. *Bioinformatics*, **29**, 15–21.
40. Love,M.I., Huber,W. and Anders,S. (2014) Moderated estimation of fold change and dispersion for RNA-seq data with DESeq2. *Genome Biol.*, **15**, 550.
41. Langmead,B., Trapnell,C., Pop,M. and Salzberg,S.L. (2009) Ultrafast and memory-efficient alignment of short DNA sequences to the human genome. *Genome Biol.*, **10**, R25.
42. Criscione,S.W., Zhang,Y., Thompson,W., Sedivy,J.M. and Neretti,N. (2014) Transcriptional landscape of repetitive elements in normal and cancer human cells. *BMC Genomics*, **15**, 583.
43. Balkwill,F. and Coussens,L.M. (2004) Cancer: an inflammatory link. *Nature*, **431**, 405–406.
44. Moynagh,P.N. (2005) TLR signalling and activation of IRFs: revisiting old friends from the NF-kappaB pathway. *Trends Immunol.*, **26**, 469–476.
45. Zhang,Y., Subbaiah,V.K., Rajagopalan,D., Tham,C.Y., Abdullah,L.N., Toh,T.B., Gong,M., Tan,T.Z., Jadhav,S.P., Pandey,A.K. *et al.* (2016) TIP60 inhibits metastasis by ablating DNMT1-SNAIL2-driven epithelial-mesenchymal transition program. *J. Mol. Cell Biol.*, **8**, 384–399.
46. Dey,A., Chitsaz,F., Abbasi,A., Misteli,T. and Ozato,K. (2003) The double bromodomain protein Brd4 binds to acetylated chromatin during interphase and mitosis. *Proc. Natl. Acad. Sci. U.S.A.*, **100**, 8758–8763.
47. Sakamaki,J.I., Wilkinson,S., Hahn,M., Tasdemir,N., O'Prey,J., Clark,W., Hedley,A., Nixon,C., Long,J.S., New,M. *et al.* (2017) Bromodomain protein BRD4 is a transcriptional repressor of autophagy and lysosomal function. *Mol. Cell*, **66**, 517–532.
48. Delmore,J.E., Issa,G.C., Lemieux,M.E., Rahl,P.B., Shi,J., Jacobs,H.M., Kastritis,E., Gilpatrick,T., Paranal,R.M., Qi,J. *et al.* (2011) BET bromodomain inhibition as a therapeutic strategy to target c-Myc. *Cell*, **146**, 904–917.
49. Filippakopoulos,P., Qi,J., Picaud,S., Shen,Y., Smith,W.B., Fedorov,O., Morse,E.M., Keates,T., Hickman,T.T., Felletar,I. *et al.* (2010) Selective inhibition of BET bromodomains. *Nature*, **468**, 1067–1073.
50. Dawson,M.A., Prinjha,R.K., Dittmann,A., Giotopoulos,G., Bantscheff,M., Chan,W.I., Robson,S.C., Chung,C.W., Hopf,C., Savitski,M.M. *et al.* (2011) Inhibition of BET recruitment to chromatin as an effective treatment for MLL-fusion leukaemia. *Nature*, **478**, 529–533.

51. Chaidos,A., Caputo,V. and Karadimitris,A. (2015) Inhibition of bromodomain and extra-terminal proteins (BET) as a potential therapeutic approach in haematological malignancies: emerging preclinical and clinical evidence. *Ther. Adv. Hematol.*, **6**, 128–141.
52. Zhao,Y., Yang,C.Y. and Wang,S. (2013) The making of I-BET762, a BET bromodomain inhibitor now in clinical development. *J. Med. Chem.*, **56**, 7498–7500.
53. Okabe,Y., Kawane,K., Akira,S., Taniguchi,T. and Nagata,S. (2005) Toll-like receptor-independent gene induction program activated by mammalian DNA escaped from apoptotic DNA degradation. *J. Exp. Med.*, **202**, 1333–1339.
54. Ma,Z. and Damania,B. (2016) The cGAS-STING defense pathway and its counteraction by viruses. *Cell Host Microbe*, **19**, 150–158.
55. Suschak,J.J., Wang,S., Fitzgerald,K.A. and Lu,S. (2016) A cGAS-independent STING/IRF7 pathway mediates the immunogenicity of DNA vaccines. *J. Immunol.*, **196**, 310–316.
56. Elsasser,S.J., Noh,K.M., Diaz,N., Allis,C.D. and Banaszynski,L.A. (2015) Histone H3.3 is required for endogenous retroviral element silencing in embryonic stem cells. *Nature*, **522**, 240–244.
57. Bulut-Karslioglu,A., De La Rosa-Velazquez,I.A., Ramirez,F., Barenboim,M., Onishi-Seebacher,M., Arand,J., Galan,C., Winter,G.E., Engist,B., Gerle,B. *et al.* (2014) Suv39h-dependent H3K9me3 marks intact retrotransposons and silences LINE elements in mouse embryonic stem cells. *Mol. Cell*, **55**, 277–290.
58. Hanahan,D. and Weinberg,R.A. (2011) Hallmarks of cancer: the next generation. *Cell*, **144**, 646–674.
59. Polk,D.B. and Peek,R.M. Jr. (2010) Helicobacter pylori: gastric cancer and beyond. *Nat. Rev. Cancer*, **10**, 403–414.
60. Balkwill,F. and Mantovani,A. (2001) Inflammation and cancer: back to Virchow? *Lancet*, **357**, 539–545.
61. Coussens,L.M. and Werb,Z. (2002) Inflammation and cancer. *Nature*, **420**, 860–867.
62. Chen,R., Alvero,A.B., Silasi,D.A., Steffensen,K.D. and Mor,G. (2008) Cancers take their Toll—the function and regulation of Toll-like receptors in cancer cells. *Oncogene*, **27**, 225–233.
63. Huang,B., Zhao,J., Unkeless,J.C., Feng,Z.H. and Xiong,H. (2008) TLR signaling by tumor and immune cells: a double-edged sword. *Oncogene*, **27**, 218–224.
64. Ilvesaro,J.M., Merrell,M.A., Swain,T.M., Davidson,J., Zayzafoon,M., Harris,K.W. and Selander,K.S. (2007) Toll like receptor-9 agonists stimulate prostate cancer invasion in vitro. *Prostate*, **67**, 774–781.
65. Ren,T., Wen,Z.K., Liu,Z.M., Liang,Y.J., Guo,Z.L. and Xu,L. (2007) Functional expression of TLR9 is associated to the metastatic potential of human lung cancer cell: functional active role of TLR9 on tumor metastasis. *Cancer Biol. Ther.*, **6**, 1704–1709.
66. Sun,Y., Jiang,X., Xu,Y., Ayrapetov,M.K., Moreau,L.A., Whetstine,J.R. and Price,B.D. (2009) Histone H3 methylation links DNA damage detection to activation of the tumour suppressor Tip60. *Nat. Cell Biol.*, **11**, 1376–1382.